Published in final edited form as:

Nature. ; 485(7400): 605–610. doi:10.1038/nature11061.

The *let-7*–Imp axis regulates ageing of the *Drosophila* testis stem-cell niche

Hila Toledano[1,†,*], **Cecilia D'Alterio**[1,*], **Benjamin Czech**[2], **Erel Levine**[3], and **D. Leanne Jones**[1]

[1]Laboratory of Genetics, The Salk Institute for Biological Studies, La Jolla, California 92037, USA

[2]Watson School of Biological Sciences, Howard Hughes Medical Institute, Cold Spring Harbor Laboratory, 1 Bungtown Road, Cold Spring Harbor, New York 11724, USA

[3]Department of Physics and FAS Center for Systems Biology, Harvard University, Cambridge, Massachusetts 02138, USA

Abstract

Adult stem cells support tissue homeostasis and repair throughout the life of an individual. During ageing, numerous intrinsic and extrinsic changes occur that result in altered stem-cell behaviour and reduced tissue maintenance and regeneration. In the *Drosophila* testis, ageing results in a marked decrease in the self-renewal factor Unpaired (Upd), leading to a concomitant loss of germline stem cells. Here we demonstrate that IGF-II messenger RNA binding protein (Imp) counteracts endogenous small interfering RNAs to stabilize *upd* (also known as *os*) RNA. However, similar to *upd*, Imp expression decreases in the hub cells of older males, which is due to the targeting of *Imp* by the heterochronic microRNA *let-7*. In the absence of Imp, *upd* mRNA therefore becomes unprotected and susceptible to degradation. Understanding the mechanistic basis for ageing-related changes in stem-cell behaviour will lead to the development of strategies to treat age-onset diseases and facilitate stem-cell-based therapies in older individuals.

Many stem cells lose the capacity for self-renewal when removed from their local microenvironment (or niche), indicating that the niche has a major role in controlling stem-cell fate[1]. Changes to the local and systemic environments occur with age that result in altered stem-cell behaviour and reduced tissue maintenance and regeneration[2,3]. The stem-cell niche in the *Drosophila* testis is located at the apical tip, where both germline stem cells

Correspondence and requests for materials should be addressed to D.L.J. (ljones@salk.edu).

†Present address: Department of Human Biology, Faculty of Natural Sciences, University of Haifa, Mount Carmel, Haifa 31905, Israel.

*These authors contributed equally to this work.

Supplementary Information is linked to the online version of the paper at www.nature.com/nature.

Author Contributions H.T., C.D. and D.L.J. designed experiments. H.T. and C.D. performed experiments. B.C. generated and analysed small RNA libraries. E.L. performed bioinformatic analysis to identify Imp-binding sequences. H.T., C.D., B.C. and D.L.J. evaluated the data and wrote the manuscript.

The small RNA libraries from the testes of 1-day-old and 30-day-old flies have been deposited in the Gene Expression Omnibus database under accession GSE37041.

The authors declare no competing financial interests.

(GSCs) and somatic cyst stem cells are in direct contact with hub cells (Fig. 1a; reviewed in ref. 4). Hub cells express the self-renewal factor Upd, which activates the JAK-STAT signalling pathway to regulate the behaviour of adjacent stem cells[5–7]. Ageing results in a progressive and significant decrease in the levels of *upd* in hub cells (Fig. 1b). However, constitutive expression of *upd* in hub cells was sufficient to block the age-related loss of GSCs[5], suggesting that mechanisms might be in place to regulate *upd* and maintain an active stem-cell niche.

To identify potential regulators of *upd*, we screened a collection of transgenic flies carrying green fluorescent protein (GFP)-tagged proteins for expression in hub cells[6]. The *Drosophila* homologue of Imp protein is expressed throughout the testis tip in young flies (Fig. 1c and Supplementary Fig. 2a)[7]; however, antibody staining revealed a decrease (~50%) in Imp expression in the hub cells of aged males (Fig. 1d and Supplementary Fig. 2b). Imp is a member of a conserved family of RNA-binding proteins that regulate RNA stability, translation and localization[8]. Given the similarity in the ageing-related decline in Imp protein and *upd* mRNA in hub cells, we proposed that Imp could be a new regulator of *upd*.

Imp acts upstream to regulate *upd* mRNA

To address whether Imp acts in hub cells to regulate *upd*, we used the bipartite *GAL4-UAS* system[9] in combination with RNA-mediated interference (RNAi) to reduce *Imp* expression exclusively in hub cells. Fluorescence *in situ* hybridization (FISH) to detect *upd* mRNA was used in combination with immunofluorescence microscopy to determine whether the loss of Imp expression affects *upd* levels. The loss of Imp specifically in hub cells resulted in reduced expression of *upd* (Fig. 1e, f (bottom), and Supplementary Fig. 2c, d), as well as a significant reduction in GSCs and hub cells (Fig. 1h, i, k and Supplementary Fig. 2e), when compared with controls. Consistent with a reduction in JAK-STAT signalling, decreased accumulation of STAT was observed when Imp levels were reduced by RNAi in hub cells (Supplementary Fig. 2f–h).

RNA-binding proteins characteristically target several RNAs; therefore, we wanted to determine whether *upd* is a physiologically relevant target of Imp. Expression of *upd* together with an *Imp* RNAi construct was sufficient to completely rescue the defects caused by reduced *Imp* expression in hub cells (Fig. 1e–k and Supplementary Fig. 2e), suggesting that Upd acts downstream of Imp to maintain GSCs and niche integrity. Importantly, the constitutive expression of *upd* alone in hub cells did not lead to an increase in GSCs in testes from 1-day-old males (*w, upd-GAL4;* 8.3 ± 0.7 (mean ± 95% confidence interval), $n = 21$, and *upd-GAL4; UAS-upd, TM2*; 8.3 ± 0.8, $n = 32$). These data suggest that Imp acts in hub cells to promote niche integrity and GSC maintenance, at least in part, by positively regulating *upd*.

If Imp acts in hub cells in adult testes to regulate *upd* mRNA, we speculated that the loss of Imp function during development might lead to a decrease in *upd* and a subsequent reduction in GSCs. Null mutations in *Imp* result in lethality at the pharate adult stage; therefore, we examined testes from third instar larvae (L3) carrying *Imp* null alleles, Imp^{7} and Imp^{8} (ref. 10). Deletion of the *Imp* locus was verified by PCR of genomic DNA

(Supplementary Fig. 3a). Combined immunofluorescence and FISH showed that although Fas3$^+$ hub cells were easily detected, the expression of *upd* was significantly reduced: 24% of *Imp*^{7} mutants (n = 67) and 15% of *Imp*^{8} mutants (n = 41) had no detectable *upd* at this stage (Fig. 1l, m). In addition, the average number of GSCs and hub cells in testes from *Imp* mutants was significantly reduced when compared with control L3 testes (Fig. 1o–p, r and Supplementary Fig. 3c–e). Notably, the re-expression of *Imp* in somatic niche cells was sufficient to rescue *upd* expression in *Imp* mutants to comparable levels to controls (Fig. 1l–n), and the reduction in the average number of GSCs and hub cells in *Imp* mutants was also reversed (Fig. 1o–q, r and Supplementary Fig. 3c–e).

Imp binds to *upd in vivo* and *in vitro*

Imp family members contain conserved KH domains that mediate direct binding to RNA targets. To determine whether Imp could associate directly with *upd* mRNA *in vivo*, testes were dissected from young flies expressing GFP-tagged Imp (Supplementary Fig. 2a)[6]. Immunoprecipitation of Imp with anti-GFP antibodies, followed by quantitative reverse transcriptase PCR (qRT–PCR) analysis, showed a significant enrichment (~208-fold) of associated *upd* mRNA relative to control antibodies (Fig. 2a). Minimal enrichment for the ubiquitously expressed RNAs *rp49* (also known as *RpL32*; ~4-fold) and *GapDH* (also known as *Gapdh1*; ~8 fold) or for the negative control *med23* (~4-fold; see Methods), was observed after Imp immunoprecipitation, indicating that the interaction between Imp and *upd* mRNA in hub cells is specific (Fig. 2a). Consistent with these observations, Imp protein and *upd* RNA co-localized in hub cells within perinuclear foci, probably ribonucleoprotein particles (Supplementary Fig. 4a).

An *in vitro* protein–RNA binding assay[11] showed that Imp associates with the *upd* 3′ untranslated region (UTR), specifically the first 250 base pairs (region 1), as no substantial binding to other portions of the *upd* 3′UTR was detected (Fig. 2b). Moreover, Imp did not bind the 5′ untranslated or coding regions of *upd* or to the *med23* 3′UTR (Fig. 2b). Notably, a putative consensus binding sequence CAUH (in which Hdenotes A, U or C) for the mammalian IMP homologues (IGF2BP1–3)[12] occurs 22 times within the *upd* 3′UTR, including a cluster of four tandem repeats within the first 35 nucleotides of region 1 (Fig. 2c). To test whether this motif mediates binding between Imp and *upd*, we removed the first 33 nucleotides to generate a sequence excluding the CAUH repeats, which resulted in a reduction in binding (Fig. 2c, compare domain 1 with domain 2). Point mutations in the third nucleotide of each motif (U = G) did not abolish the binding (Fig. 2c, domain 1*); however, point mutations in the consensus motif of *MRPL9* RNA, a target of mammalian IGF2BPs, also did not abolish binding[12], suggesting that secondary structures probably mediate the association between IGFBP family members and their target RNAs. Altogether, our data identify the first 33 base pairs of the *upd* 3′UTR as a putative target sequence for Imp, and support our observations that Imp associates specifically with *upd in vivo* (Fig. 2a, c).

To gain further insight into the mechanism by which Imp regulates *upd*, a GFP reporter was constructed that contained the 3′UTR from either *upd* or *med23* (Fig. 2d). Transcript levels for *gfp* were fivefold higher in *Drosophila* Schneider (S2) cells that co-expressed Imp with

the *gfp-upd*-3′UTR reporter than in cells that co-expressed Imp with the *gfp-med23*-3′UTR reporter (Fig. 2d). The significant increase in reporter mRNA levels indicates that it is likely that Imp regulates *upd* mRNA stability.

Imp counters targeting of *upd* by endo-siRNAs

RNA-binding proteins, including mammalian IGF2BP1 (refs 13, 14), have been shown to counter microRNA (miRNA)-mediated targeting of mRNAs. However, no consensus miRNA seeds were located within the first 34 base pairs of domain 1 of the *upd* 3′UTR (Fig. 2c). We speculated that if Imp binding blocks small RNA-mediated degradation of *upd*, polyadenylated, cleaved *upd* degradation intermediates would be detected in the testes of older males, when Imp expression in hub cells is reduced (Fig. 1d). Using a modified rapid amplification of complementary DNA ends (RACE) technique we identified a specific cleavage product starting at nucleotide 33 of the *upd* 3′UTR in the testes of 30-day-old flies (Fig. 2e), but not in RNA extracts from the testes of 1-day-old males. Importantly, the same degradation product of *upd* was also detected in the testes of young flies when Imp was specifically depleted from hub cells using RNAi-mediated knockdown. As a positive control, we detected the *esi-2*-mediated cleavage product of *mus308* (ref. 15) in testes from both 1- and 30-day-old flies.

To test whether small RNAs might mediate *upd* cleavage, we cloned and deep-sequenced small RNA libraries generated from the testes of 1- and 30-day-old flies. Although no small RNAs with exact pairing to the *upd* degradation product were identified, two short interfering RNAs (siRNAs; termed *siRNA1* and *siRNA2*) with high sequence complementarity to the predicted target site in the *upd* 3′UTR were present in the testis library generated from 30-day-old males (Fig. 2e and Supplementary Table 1). Using qRT–PCR for mature small RNAs, we found that the *siRNA2* levels in the testes, relative to the levels of the control small RNAs *bantam* and *mir-184*, were similar in young and old males (deep sequencing analysis demonstrated that expression of these two control miRNAs did not change with age). The source of *siRNA2* is the *gypsy5* transposon, which is inserted at several loci throughout the fly genome and is conserved in numerous *Drosophila* species.

To gain further insight into the mechanism by which Imp and *siRNA2* regulate *upd*, we investigated the levels of the *upd* GFP reporter (*gfp-upd*-3′UTR) in the presence or absence of Imp and *siRNA2* in S2 cells. To generate a reporter that should not be susceptible to siRNA-mediated degradation, we mutated the cleavage site in the *upd* 3′UTR that was identified by RACE (^{32}AUU = CGG; *gfp-upd*-3′UTR^{mut}). Cells were transfected with either of the GFP reporter constructs, with or without haemagglutinin-tagged Imp (Imp–HA), and subsequently transfected with *siRNA2; gfp* expression was quantified by qRT–PCR.

The co-expression of *siRNA2* and the *gfp-upd*-3′UTR reporter resulted in a significant decrease in *gfp* transcript levels (Fig. 2f). Conversely, the co-expression of Imp blocked *siRNA2*-mediated reduction of *gfp* mRNA such that *gfp* levels were higher than in control cells (Fig. 2f). Furthermore, mutation of the putative cleavage site rendered the *upd* 3′UTR resistant to *siRNA2*-mediated degradation (Fig. 2f). These data, in combination with the *in vitro* binding data, suggest that Imp binds to and protects the *upd* 3′UTR from endogenous

and exogenous *siRNA2* in S2 cells. Thus, endo-*siRNA2* is a bona fide candidate that could direct *upd* degradation when Imp is absent or its levels are reduced, although targeting by other small RNAs cannot be excluded.

In *Drosophila*, Argonaute-1 (AGO1) is the principle acceptor of miRNAs and primarily regulates targets in a cleavage-independent mode, whereas AGO2 is preferentially loaded with siRNAs and typically regulates targets by mRNA cleavage[16] (reviewed in refs 17, 18). AGO2 expression was detected throughout the tip of the testis, as verified by immunostaining of testes from transgenic flies expressing 3×Flag-HA-tagged AGO2 (ref. 15; Fig. 3a, b). To test whether AGO2 binds to *upd* mRNA *in vivo*, thereby potentially regulating *upd* levels directly, testes were dissected from aged (30-day-old) 3×Flag–HA–AGO2 males. Immunoprecipitation of AGO2, followed by qRT–PCR, showed significant enrichment (~102-fold) of *upd* mRNA bound to AGO2 (Fig. 3c). Negligible binding of a negative control, *rp49*, to AGO2 was detected, suggesting specific association of AGO2 with *upd* mRNA *in vivo* and supporting our previous findings that *upd* is probably targeted by the siRNA pathway (Fig. 3c).

To test whether Imp can impede the binding of AGO2 to the *upd* 3′UTR, S2 cells stably expressing Flag-tagged AGO2 (ref. 19) were transfected with the *gfp-upd*-3′UTR reporter. Consistent with our previous observations, transcript levels of *gfp-upd*-3′UTR increased ~18-fold when Imp was co-expressed (Fig. 2d and Supplementary Fig. 5b). Despite increases in the overall levels of *gfp* mRNA, the presence of Imp markedly reduced the association of AGO2 with the *upd* 3′UTR (Fig. 3d), indicating that Imp antagonizes the ability of AGO2 to bind the *upd* 3′UTR.

Similar to the AGO family, *Drosophila* encodes two Dicer proteins that seem to have distinct roles in small RNA biogenesis. Dicer-1 (Dcr-1) is essential for the generation of miRNAs, and Dcr-2 is required for siRNA production from exogenous and endogenous sources[16] (reviewed in refs 17, 18). If siRNAs were involved in *upd* degradation in older males, we predicted that the loss of *Dcr-2* would suppress the ageing-related decline in *upd* and GSCs. Consistent with a role for *Dcr-2* in the generation of siRNAs, *siRNA2* levels were significantly reduced in *Dcr-2* homozygous mutants relative to heterozygous controls (Fig. 3e). Testes from 30- and 45-day-old *Dcr-2* mutant flies showed increased levels of *upd* by qRT–PCR when compared with controls. Whereas a ~90% reduction of *upd* is observed in the testes from aged *Dcr-2* heterozygous controls, we observed only a ~45% reduction in *upd* in testes from age-matched, *Dcr-2* homozygous mutants (Fig. 3f), indicating that *upd* levels are higher when *Dcr-2* function is compromised. Furthermore, the testes from aged *Dcr-2* mutants contained more GSCs, on average, when compared with controls (Supplementary Fig. 5c–h). Conversely, the forced expression of *Dcr-2* in hub cells resulted in a reduction in the average number of GSCs (Supplementary Fig. 5i–j, l) and led to a significant reduction in *upd* levels, as detected using qRT–PCR and combined immunofluorescence and FISH, which seemed to be specific, as no significant change in *Imp* transcript levels was observed (Fig. 3g and Supplementary Fig. 5m, n). Expression of Imp in combination with Dcr-2 resulted in a significant increase in *upd* levels (Fig. 3g), with a concomitant increase in the average number of GSCs (Supplementary Fig. 5i–l). These observations indicate that Imp can counter the decrease in *upd* levels resulting from forced

Dcr-2 expression, providing further evidence that Imp protects *upd* from targeted degradation by the siRNA pathway.

let-7 targets Imp in the *Drosophila* testis

Our data suggest that Imp has a role in stabilizing *upd* in hub cells; therefore, the ageing-related decline in Imp would be a major contributing factor to the decrease in *upd* mRNA in the hub cells of aged males. To investigate the mechanism that leads to the decline in Imp expression with age, we examined the *Imp* 3′UTR for potential instability elements. Within the first 160 base pairs there is a canonical seed sequence for the heterochronic miRNA *let-7* (Fig. 4a). Expression of a reporter gene under the control of the *let-7* promoter showed that *let-7* expression increases in hub cells of ageing males (Fig. 4b, c), which was confirmed by *let-7* FISH of testes from aged males (Supplementary Fig. 6a–d). In addition, mature *let-7* miRNA was enriched twofold in the testes from 30-day-old flies, relative to 1-day-old males (Fig. 4d). Therefore, an age-related increase in *let-7* is one mechanism by which *Imp* expression could be regulated in an ageing-dependent manner in testes from older males.

Consistent with these observations, the forced expression of *let-7* specifically in hub cells led to a decrease in Imp (Fig. 4e, f, insets). In addition, *let-7* expression in S2 cells reduced the levels of a heterologous *gfp-Imp*-3′UTR^{WT} reporter. S2 cells were transfected with a *let-7* mimic or with negative control miRNA, and *gfp* expression was quantified by qRT–PCR. There was a 70% reduction in *gfp-Imp*-3′UTR^{WT} expression in the presence of *let-7*, relative to control miRNA (Fig. 4g). A *gfp-Imp*-3′UTR^{mut} reporter with mutations in the canonical seed for *let-7* (at nucleotide 137) was unaffected by *let-7* expression, indicating that mutation of the *let-7* seed rendered the RNA resistant to degradation. These data confirm that *let-7* can destabilize *Imp* through sequences in the 3′UTR (Fig. 4g). However, further increasing the levels of *let-7* resulted in a decrease in *gfp* expression from the mutated 3′UTR, indicating that other, putative *let-7* seeds in the *Imp* 3′UTR can be targeted by *let-7* (Fig. 4g and Supplementary Fig. 6e).

If the age-related decrease in Imp contributes to a decline in *upd* and subsequent loss of GSCs, we proposed that re-expression of *Imp* in hub cells would rescue the ageing-related decrease in *upd*. Therefore, flies in which *Imp* was constitutively expressed in hub cells were aged, and *upd* levels were quantified by qRT–PCR. The expression of an Imp construct containing a truncated 3′UTR (Imp-KH–HA) lacking *let-7* target sequences specifically in hub cells was sufficient to suppress the ageing-related decline in *upd*, with concomitant maintenance of GSCs (Fig. 4h, j, k and Supplementary Fig. 6f), similar to what was observed by re-expressing *upd* in the hub cells of aged males[5,33]. Maintenance of Imp-KH–HA expression in aged males was verified by staining with an anti-HA antibody (Fig. 4j, inset). Conversely, the expression of an *Imp* construct that is susceptible to degradation by *let-7* (*Imp*^{T21}) did not lead to an accumulation of *Imp* in the testes of 30- and 50-day-old flies, as levels were similar to the levels of endogenous *Imp* at later time points (Supplementary Fig. 6g)[20]. Consequently, the expression of this construct was not sufficient to block the ageing-related decline in GSCs (Fig. 4h, i and Supplementary Fig. 6f). These data indicate that *let-7*-mediated regulation of *Imp* contributes to the decline in Imp protein in older flies, and supports a model in which an ageing-related decline in Imp, mediated by

let-7, exposes *upd* to degradation by siRNAs (Supplementary Fig. 1). Thus, both the miRNA and siRNA pathways act upstream to regulate the ageing of the testis stem-cell niche by generating *let-7* and *siRNA2*, which target *Imp* and *upd*, respectively.

Drosophila has proven to be a valuable model system for investigating ageing-related changes in stem-cell behaviour[21]. Cell autonomous and extrinsic changes contribute to altered stem-cell activity; thus, determining the mechanisms underlying the ageing-related decline of self-renewal factors, such as the cytokine-like factor Upd, may provide insight into strategies to maintain optimal niche function.

Our data indicate that Imp can regulate gene expression by promoting the stability of selected RNA targets by countering inhibitory small RNAs. Therefore, rescue of the aged niche by *Imp* expression may be a consequence of effects on Imp targets, in addition to *upd*, in somatic niche cells. Furthermore, as Imp is expressed in germ cells, it could also act in an autonomous manner to regulate the maintenance of GSCs. The canonical *let-7* seed in the *Imp* 3′UTR is conserved in closely related species, and reports have predicted that the *let-7* family of miRNAs target mammalian Imp homologues (IGF2BP1–3)[22]. Given the broad role of the *let-7* family in ageing[23], stem cells[24–28], cancer[29,30] and metabolism[31], the regulation of Imp by *let-7* may be an important, conserved mechanism in numerous physiological processes.

Non-coding RNAs can ensure biological robustness and provide a buffer against relatively small fluctuations in a system[32]. However, after a considerable change, a molecular switch is flipped, which allows a biological event to proceed unimpeded. In our model, Imp preserves niche function in young flies until a time at which miRNAs and siRNAs act together to trigger an ‘ageing’ switch that leads to a definitive decline in *upd* and, ultimately, in stem-cell maintenance (Supplementary Fig. 1). Therefore, targeting signalling pathways at several levels using RNA-based mechanisms will probably prove to be a prevalent theme to ensure robustness in complex biological systems.

METHODS

Drosophila stocks and genotypes

Wild-type flies were *Oregon R*. Additional strains used were: *upd-GAL4, UAS-gfp* (E. Bach); *upd-GAL4* (T. Xie); w^{-}*;UAS-upd, TM2* (D. Harrison); *w; let-7C*^{GK1}/CyO and *UAS-let7*$^{701.12.9}$ (N. Sokol[35]); 3×Flag/HA–AGO2 (G. Hannon[15]); *Imp*^{CB04573} (A. Spradling[6]); *8-156-GAL4* (U. Heberlein[36]); *UAS-Imp*^{T21} (P Macdonald[20]); *UAS-Imp HA-KH1 3-3* (from T. Hays[33]; *UAS-Imp(RNAi)* (Vienna *Drosophila* RNAi Center (VDRC) stock number 20322); and *UAS-gfp*^{nls} (Bloomington *Drosophila* Stock Center (BDSC) number 4775).

Imp^{7} and *Imp*^{8} were gifts from D. St Johnston[10]. EP(X)760 (w^{1118}, P{w^{+mc} = EP}*Imp*^{EP760}; BDSC number 17294) was used as a control for *Imp*^{7} and *Imp*^{8} alleles. *Imp*^{7} and *Imp*^{8} hemizygous larvae (L3) were obtained by crossing *Imp*^{7}/FM0 or *Imp*^{8}/FM0 females with FM7,*KrGAL4, UAS-gfp* males (BDSC). L3 mutants were selected against GFP. Specifically, *Imp*^{7}/FM7, *KrGAL4, UAS-gfp; 8-156-GAL4* or *Imp*^{8}/FM7, *KrGAL4, UAS-*

gfp; 8-156-GAL4 females were crossed to $w^{-}/Y;+;$ *UAS-Imp*^{T21} males, and non-GFP L3 male progeny were selected.

UAS-Dcr-2 (VDRC number 60008) and *yw, eyFLP; FRT42D, Dcr-2*^{L811fsX} were gifts from R.W. Carthew[16]. Heterozygous flies were obtained by out-crossing to *w; FRT42D* (BDSC number 1802). An independent *Dcr-2* mutant background was obtained by crossing *Df(2R)BSC45w*$^{+}$ *mC/SM6a* (*Dcr-2* deficiency chromosome; BDSC number 7441) with *y, w, eyFLP; FRT42D, Dcr-2*^{L811fsX}. Heterozygous flies were obtained by out-crossing *Df(2R)BSC45, w+ mC/SM6a* to *w; FRT42D*.

Antibodies

Primary antibodies for immunofluorescence were as follows: rabbit anti-Imp (1:600, gift from P. M. Macdonald[20]), mouse anti-HA (1:800, Covance), rabbit anti β-galactosidase (1:2,000, Cappel), rabbit anti-GFP (1:5,000, Invitrogen), rabbit anti-Vasa (1:3,000, gift from P. Lasko), rabbit anti-STAT (1:800, gift from D. Montell); mouse anti-Fas3 (1:50), rat anti-DEcad (1:20) and rat anti-DNcad (1:20) were obtained from the Developmental Studies Hybridoma Bank, developed under the auspices of the National Institute of Child Health and Human Development and maintained by the University of Iowa, Department of Biological Sciences. Secondary antibodies were obtained from Invitrogen.

Combined FISH and immunofluorescence

For *let-7* miRNA detection, testes were dissected, squashed onto slides[37], and incubated with primary antibodies using PBT (diethylpyrocarbonate PBS, 0.1% Tween 20) and PBTHR solutions[34]. After washes and secondary antibodies, slides were treated with proteinase K for 3 min, rinsed and post-fixed in 10% formaldehyde. Slides were then treated according to the manufacturer's recommendations for miRNA *in situ* (Exiqon). Slides were hybridized with 40 nM *let-7* LNA-digoxigenin (DIG) probe for 1 h at 50 °C with Exiqon hybridization buffer in a humid chamber. *let-7* FISH detection signal and mounting was performed similar to *upd*.

Generation of DNA constructs

The nucleotide numbers of the following sequences refer to their numbers in the 3′UTRs/5′UTRs or open reading frames (ORF), as shown on FlyBase. All point mutations described were generated by site-directed mutagenesis (Stratagene). pBS-*upd* was a gift from D.A. Harrison[38]. pAc5.1-*Imp*-HA and pBS-*Imp*-HA were produced by PCR of *Imp*-RB ORF using *Imp* cDNA (expressed sequence tag (EST) clone SD07045) as a template. pBS-*upd*-3′UTR or pBS-*med23*-3′UTR was produced by PCR of the *upd* 3′UTR (nucleotides 73–707) or *med23* 3′UTR (nucleotides 791–1391) and ligated into pBS. To generate pAc5.1-*gfp-upd*-3′UTR and pAc5.1-*gfp-upd*-3′UTR^{mut} (^{32}ATT = CGG), nucleotides 1–737 of the *upd* 3′UTR were ligated into pAc5.1 following the *gfp* ORF. pBS-*upd*-5′UTR and pBS-*upd*-coding were produced by PCR of the *upd* 5′UTR (nucleotides 1–224 of *os*-RA) or *upd* coding region (nucleotides 29–1191 of *os* ORF) and ligated into pBS. Region 1 (nucleotides 4–243), region 2 (nucleotides 228–468), region 3 (nucleotides 443–737), domain 1 (nucleotides 1–152) and domain 2 (nucleotides 33–152) of the *upd* 3′UTR were amplified by PCR and ligated into pBS. Domain 1* of the *upd* 3′UTR was generated by four point

mutations (U8G, U17G, U23G and U33G). To generate pAc5.1-*gfp-Imp*-3′UTR^{WT}, *Imp-RB* 3′UTR (nucleotides 45–781) was amplified by PCR and then ligated into pGEM T-Easy (Promega). In pAc5.1-*gfp-Imp*-3′UTR^{MUT}, the *let-7* seed was disrupted by five tandem point mutations (^{149}TACCT = CGTTC). pGEM T-Easy-*Imp* 3′UTR wild-type and mutant were then digested with NotI and ligated downstream of the *gfp* coding region in pAc5.1-*gfp*. The sequence of all DNA constructs described above was verified by DNA sequencing.

RNA–protein binding assay and western blotting

Biotin-labelled RNA was transcribed *in vitro* from cDNAs cloned into pBS using T7 RNA polymerase. The RNA concentration was measured, and an equal number of RNA molecules (according to size) was assayed for protein binding. Imp–HA was translated *in vitro* using the TNT Coupled Reticulocyte Lysate System (Promega), and 5 μl of the translation mixture was mixed with biotin-labelled RNA. Binding assays were performed as described[12]. Associated protein complexes were separated on 10% SDS–PAGE gels, followed by western blotting according to standard procedures. Antibodies for western analysis (1:1,000) were: mouse anti-Flag and mouse anti-α-tubulin (Sigma), mouse anti-HA (Covance) and mouse anti-GFP (Clontech).

In silico examination of the *upd* 3′UTR, 5′UTR and coding regions showed that the *upd* 3′UTR contains an abundance of AU-rich sequences. Annotated *Drosophila* 3′UTRs were surveyed for the AU/CG ratio, and identified the *med23* 3′UTR as one that should not be recognized by Imp, owing to equal AU/CG ratios. Statistical analysis of possible Imp-binding sequences was done in MATLAB (Mathwork). All sequences that bound Imp *in vitro* were analysed by Meme[39] to search for sequence motifs. Alignment based on locally stable RNA structure was performed by LocARNA (the Vienna package: http://rna.tbi.univie.ac.at/).

S2 cell culture and transfection

S2 adherent cells were cultured in Schneider's *Drosophila* medium and supplemented with 10% heat-inactivated fetal bovine serum (Invitrogen). Each experiment was done at least three times and each transfection was performed in triplicate. Plasmids were transfected according to the manufacturer's recommendations (Fugene HD, Roche). For GFP-3′UTR dependent assays, cells were transfected with pBS-actin-*GAL4* (obtained from T. Volk) and with either *UAS-gfp-upd*-3′UTR or *UAS-gfp-med23*-3′UTR and with 1 μg pAC 5.1 empty vector or pAC 5.1-ImpHA. Cells were collected 20–26 h after transfection and RNA was extracted with the RNeasy kit (Qiagen) and used for qRT–PCR. *gfp* levels were quantified relative to *GAL4* to account for transfection efficiency.

To test the activity of *siRNA2* functionally, S2 cells were transfected with pAc5.1-*gfp-upd*-3′UTR, with either pAC 5.1 empty vector or pAc5.1-*Imp*-HA, or with pAc5.1-*gfp-upd*-3′UTR^{mut} (^{32}ATT = CGG). Thirty-six hours after transfection, each plate was split into two. One plate was transfected with 100 nM annealed oligonucleotides for *siRNA2* (guide sequence: 5′-UGAGGGGAAAU UGGAGGGGGU-3′, passenger sequence: 5′-CCCCUCCAAUUUCCCUUUU UU-3′) using HighPerfect (Qiagen). Cells were collected

20–26 h after second transfection and used for qRT–PCR. *gfp* levels were quantified relative to *rp49* RNA levels. Each transfection was performed in triplicate.

For the *gfp* or *let-7* reporter assay, cells were transfected with reporter construct of *gfp-Imp*-3′UTR^{WT} or *gfp-Imp*-3′UTR^{mut}. Twenty-four hours after transfection, cells from each transfection were reseeded in 6-cm plates and transfected with 50 or 100 nM of synthetic pre-miRNAs to gain expression of *dme-miR-let-7* or negative control miRNA (Applied Biosystems) using HiPerfect (Qiagen). Cells were collected 48 h after miRNA transfection and total RNA was extracted with TRIzol (Invitrogen). For each sample we used qRT–PCR to measure *let-7* and *bantam* miRNA expression with Taqman probes for mature miRNA and *gfp* reporter levels using primers for *gfp* and *GapDH*.

RNA–protein co-immunoprecipitation

Magna RIP RNA-binding protein immunoprecipitation kit (Millipore) was used to precipitate GFP-tagged Imp (Imp–GFP) or 3×Flag/HA-tagged AGO2 and associated RNA from testes. Testes from ~1,500 males were dissected on dry ice, and homogenized in RNA immunoprecipitation lysis buffer. Each lysate was divided into two samples; one was used for immunoprecipitation with either rabbit anti-GFP (Clontech) or mouse anti-Flag (Sigma) antibodies, and the second was used with control rabbit or mouse IgG according to the manufacturer's instructions. RNA was phenol–chloroform precipitated from samples and from input (10% of control immunoprecipitate input before washes). Input RNA was used to establish a standard curve to calculate the percentage of precipitated RNA. Complementary DNA was prepared with random hexamer primers, followed by qRT–PCR.

For AGO2 RNA immunoprecipitation, S2 cells stably expressing Flag–AGO2 (gift from N. Perrimon[19]) were transfected with pAc5.1-*gfp-upd*-3′UTR with and without pAc5.1-*Imp*. Thirty-six hours after transfection, protein extracts from each plate were split into two samples; mouse anti-Flag antibodies (Sigma) or anti-mouse IgG were used for immunoprecipitation. To quantify bound RNAs, qRT–PCR was performed with primers for *gfp, rp49* and *Imp* (primers sequence below). Each transfection was performed in triplicate.

qRT–PCR

S2 cells were washed with PBS and testes from ~125 males were dissected in PBS and immediately frozen on dry ice. Cells or testes were homogenized in RLT buffer from the RNeasy kit (Qiagen), and RNA was extracted according to kit instructions. RNA was quantified and 1 μg was treated with DNaseI (Promega) and reverse-transcribed with random hexamer mixture and SuperScript III (Invitrogen), according to instructions. Quantitative PCR was carried out in 7900HT Fast Real-Time PCR System using SYBR Green PCR Master mix (Applied Biosystems). We used the $\Delta\Delta C_T$ method[40], and the efficiency of the target and the reference amplification was approximately equal. Specific primers for qRT–PCR of testes were: *upd* forward, 5′-CCTCCACACGCACAACTACAAG-3′, reverse, 5′-AGCTGGCCACGTAAGTTTGC-3′; *Imp* forward, 5′-GGTGGGCCGTATCATTGG-3′, reverse, 5′-TCACGCGCTGCAATTCC-3′; *med23* forward, 5′-TCAGCGTGGTGACCGAGTAC-3′, reverse, 5′-CCGATCAGGTGCTGGTTGT-3′; *rp49* forward, 5′-ATCGATATGCTAAGCTGTCGC-3′, reverse, 5′-

TGTCGATACCCTTGGGCTTG-3′. See ref. 41 for *GapDH* primer. For S2 cells, specific primers were: *GAL4* forward, 5′-GCAACGGTCCGAACCTCA-3′, reverse, 5′-GAGGCAATTGGTTGTGAAAGC-3′; *gfp* forward, 5′-TCCGCCCTGAGCAAAGAC-3′, reverse, 5′-GAACTCCAGCAGGACCATGTG-3′. Reactions were performed in triplicate and averaged, and the transcript expression level was quantified using the relative C_T method[40] and normalized to the level of *GapDH* transcript in testes and to the level of *GAL4* in S2 cells (to correct for transfection efficiency). To quantify small RNAs, total RNA from S2 cells and from testes was extracted using TRIzol (Invitrogen), and cDNA was prepared with small RNA-specific reverse-transcription primers for *let-7, siRNA2* or *bantam* (Applied Biosystems). Small RNA levels were measured using a Taqman-specific microRNA probe. Both *let-7* and *siRNA2* levels were normalized relative to *bantam*, which did not change with age according to the deep sequencing data.

Statistics

For quantification of cell number (GSC or hub cells) and for densitometric analysis of pixel intensity, the mean ± 95% confidence interval and the number (*n*) of testes examined are shown. *P* values were generated after a two-tailed Student's *t*-test.

For qRT–PCR, one of at least three representative experiments is shown (mean ± s.d. from triplicate measurements). *P* values were generated after a two-tailed Student's *t*-test was used to compare ΔC_T between time points or genotypes across three independent biological replicates[42].

Cleavage site mapping for endo-siRNA targets

Testes from 1- or 30-day-old OreR or 10-day-old *Imp(RNAi)* (*w*$^-$*, upd-GAL4, UAS-gfp; UAS-Imp(RNAi)*) or control (*w*$^-$*, upd-GAL4, UAS-gfp* outcrossed to w^{1118}) males (~600 testes for each time point) were collected on dry ice. Total RNA was extracted using TRIzol (Invitrogen) according to the manufacturer's protocol. Fifteen micrograms of total RNA were used as starting material. PolyA RNA was isolated with the Dynabeads mRNA purification kit (Invitrogen). Ligation of an RNA adaptor, reverse transcription using the GeneRacer oligo (dT) primer and 5′ RACE-PCR were performed according to the manufacturer's instructions (GeneRacer kit, Invitrogen). *upd* 5′ RACE-PCR was carried out using the GeneRacer 5′ primer (5′-CGACTGGAGCACGAGGACACTGA-3′) and an *upd* gene-specific reverse primer (5′-TAGTACTCGATGCGGGTGCGGAATG-3′), followed by one round of nested PCR using the GeneRacer 5′ nested primer (5′-GGACACTGACATGGACTGAAGGAGTA-3′) and a nested primer specific to *upd* (5′-CGGCAACTGCAGATTGTGGTTTCGT-3′). PCR products were gel purified and cloned into pCR4Blunt-TOPO (Invitrogen). Fifteen clones were sequenced with T7 primer and subjected to further analysis. The *esi-2*-mediated cleavage product of *mus308* was detected as described[15].

Small RNA libraries

Total RNA from the testes of 1,005 (1-day-old) and 1,018 (30-day-old) wild-type (OreR) males was isolated using TRIzol (Invitrogen). Small RNAs (19–28 nucleotides) were cloned as described[43]. Libraries were sequenced in-house using the Illumina GAII sequencing

platform. Obtained sequences were deposited in the Gene Expression Omnibus database under accession GSE3704.

The analysis of small RNA libraries was performed as described[20]. Illumina reads were stripped of the 3′ linker, collapsed, and the resulting small RNA sequences were matched without mismatches to the *Drosophila* release 5 genome. Only reads that met these conditions were subjected to further analyses. All reads between 20 and 22 nucleotides in size were extracted bioinformatically regardless of their annotations. Using a custom Perl script, these sequences were mapped against the predicted cleavage site at nucleotide 33 within the 3′UTR of *upd*, allowing up to six mismatches between the target site and nucleotides 2 to 18 of the small RNA (all mapping results are shown in Supplementary Table 1). Our search was focused on nucleotides 2–18 because previous studies suggested that pairing of the 5′ terminal nucleotide of the small RNA with its target is not required for efficient silencing. Furthermore, several mismatches between the 3′ end of the small RNA and the target site can be tolerated for target regulation[44,45].

Supplementary Material

Refer to Web version on PubMed Central for supplementary material.

Acknowledgments

We are grateful to D. St Johnston, W. Chia, P. Macdonald, R. Carthew, E. Bach, D. Harrison, T. Volk, U. Heberlein, A. Spradling, J. Kadonaga, G. Hannon, T. Hays, N. Sokol, H. Siomi and P. Lasko for reagents and fly stocks, to C. Doe, R. Hans, G. Volohonsky, T. Juven-Gershon, A. Pasquinelli, R. Zhou and S. Aigner for guidance on methods used in this manuscript, to O. Tam for computational support, and to C. Koehler for technical assistance. This work was supported by the G. Harold and Leila Y. Mathers Charitable Foundation, the Ellison Medical Foundation, the Emerald Foundation, the American Federation for Aging Research, and the National Institutes of Health (to D.L.J.). B.C. is supported by a PhD fellowship from the Boehringer Ingelheim Fonds. E.L. is supported by the National Science Foundation.

References

1. Schofield R. The relationship between the spleen colony-forming cell and the haemopoietic stem cell. Blood Cells. 1978; 4:7–25. [PubMed: 747780]
2. Jones DL, Rando TA. Emerging models and paradigms for stem cell ageing. Nature Cell Biol. 2011; 13:506–512. [PubMed: 21540846]
3. Voog J, Jones DL. Stem cells and the Niche: a dynamic duo. Cell Stem Cell. 2010; 6:103–115. [PubMed: 20144784]
4. Fuller, MT. The Development of *Drosophila Melanogaster*. Bate, M.; Martinez-Arias, A., editors. Cold Spring Harbor Laboratory Press; 1993. p. 71-147.
5. Boyle M, Wong C, Rocha M, Jones DL. Decline in self-renewal factors contributes to aging of the stem cell niche in the *Drosophila* testis. Cell Stem Cell. 2007; 1:470–478. [PubMed: 18371382]
6. Buszczak M, et al. The carnegie protein trap library: a versatile tool for *Drosophila* developmental studies. Genetics. 2007; 175:1505–1531. [PubMed: 17194782]
7. Fabrizio JJ, et al. Imp (IGF-II mRNA-binding protein) is expressed during spermatogenesis in *Drosophila melanogaster*. Fly. 2008; 2:47–48. [PubMed: 18820448]
8. Yisraeli JK. VICKZ proteins: a multi-talented family of regulatory RNA-binding proteins. Biol. Cell. 2005; 97:87–96. [PubMed: 15601260]
9. Brand AH, Manoukian AS, Perrimon N. Ectopic expression in *Drosophila*. Methods Cell Biol. 1994; 44:635–654. [PubMed: 7707973]

10. Munro TP, Kwon S, Schnapp BJ, St Johnston D. A repeated IMP-binding motif controls oskar mRNA translation and anchoring independently of *Drosophila melanogaster* IMP. J. Cell Biol. 2006; 172:577–588. [PubMed: 16476777]
11. Nabel-Rosen H, Dorevitch N, Reuveny A, Volk T. The balance between two isoforms of the *Drosophila* RNA-binding protein how controls tendon cell differentiation. Mol. Cell. 1999; 4:573–584. [PubMed: 10549289]
12. Hafner M, et al. Transcriptome-wide identification of RNA-binding protein and microRNA target sites by PAR-CLIP. Cell. 2010; 141:129–141. [PubMed: 20371350]
13. Bhattacharyya SN, Habermacher R, Martine U, Closs EI, Filipowicz W. Relief of microRNA-mediated translational repression in human cells subjected to stress. Cell. 2006; 125:1111–1124. [PubMed: 16777601]
14. Elcheva I, Goswami S, Noubissi FK, Spiegelman V. SCRD-BP protects the coding region of βTrCP1 mRNA from miR-183-mediated degradation. Mol. Cell. 2009; 35:240–246. [PubMed: 19647520]
15. Czech B, et al. An endogenous small interfering RNA pathway in *Drosophila*. Nature. 2008; 453:798–802. [PubMed: 18463631]
16. Lee YS, et al. Distinct roles for *Drosophila* Dicer-1 and Dicer-2 in the siRNA/miRNA silencing pathways. Cell. 2004; 117:69–81. [PubMed: 15066283]
17. Carthew RW, Sontheimer EJ. Origins and mechanisms of miRNAs and siRNAs. Cell. 2009; 136:642–655. [PubMed: 19239886]
18. Golden DE, Gerbasi VR, Sontheimer EJ. An inside job for siRNAs. Mol. Cell. 2008; 31:309–312. [PubMed: 18691963]
19. Czech B, et al. Hierarchical rules for Argonaute loading in *Drosophila*. Mol. Cell. 2009; 36:445–456. [PubMed: 19917252]
20. Geng C, Macdonald P. MImp associates with squid and Hrp48 and contributes to localized expression of gurken in the oocyte. Mol. Cell. Biol. 2006; 26:9508–9516. [PubMed: 17030623]
21. Wang L, Jones DL. The effects of aging on stem cell behavior in Drosophila. Exp. Gerontol. 2010; 46:340–344. [PubMed: 20971182]
22. Boyerinas B, et al. Identification of let-7-regulated oncofetal genes. Cancer Res. 2008; 68:2587–2591. [PubMed: 18413726]
23. Nishino J, Kim I, Chada K, Morrison SJ. Hmga2 promotes neural stem cell self-renewal in young but not old mice by reducing$p16^{Ink4a}$ and$p19^{Arf}$ Expression. Cell. 2008; 135:227–239. [PubMed: 18957199]
24. Zhao C, et al. MicroRNA *let-7b* regulates neural stem cell proliferation and differentiation by targeting nuclear receptor TLX signaling. Proc. Natl Acad. Sci. USA. 2010; 107:1876–1881. [PubMed: 20133835]
25. Landgraf P, et al. A mammalian microRNA expression atlas based on small RNA library sequencing. Cell. 2007; 129:1401–1414. [PubMed: 17604727]
26. Chen C, et al. Defining embryonic stem cell identity using differentiation-related microRNAs and their potential targets. Mamm. Genome. 2007; 18:316–327. [PubMed: 17610011]
27. Rybak A, Fuchs H, Smirnova L, Brandt C, Pohl EE, Nitsch R, Wulczyn FG. A feedback loop comprising *lin-28* and *let-7* controls pre-*let-7* maturation during neural stem-cell commitment. Nature Cell Biol. 2008; 10:987–993. [PubMed: 18604195]
28. Melton C, Judson RL, Blelloch R. Opposing microRNA families regulate self-renewal in mouse embryonic stem cells. Nature. 2010; 463:621–626. [PubMed: 20054295]
29. Iliopoulos D, Hirsch HA, Struhl K. An epigenetic switch involving NF-κB, Lin28, let-7 microRNA, and IL6 links inflammation to cell transformation. Cell. 2009; 139:693–706. [PubMed: 19878981]
30. Boyerinas B, Park SM, Hau A, Murmann AE, Peter ME. The role of let-7 in cell differentiation and cancer. Endocr Relat Cancer. 2010; 17:F19–F36. [PubMed: 19779035]
31. Zhu H, et al. The *Lin28/let-7* axis regulates glucose metabolism. Cell. 2011; 147:81–94. [PubMed: 21962509]

32. Li X, Cassidy JJ, Reinke CA, Fischboeck S, Carthew RW. A microRNA imparts robustness against environmental fluctuation during development. Cell. 2009; 137:273–282. [PubMed: 19379693]
33. Boylan KL, et al. Motility screen identifies *Drosophila* IGF-II mRNA-binding protein–zipcode-binding protein acting in oogenesis and synaptogenesis. PLoS Genet. 2008; 4:e36. [PubMed: 18282112]
34. Kitadate Y, et al. Boss/Sev signaling from germline to soma restricts germline-stem-cell-niche formation in the anterior region of *Drosophila* male gonads. Dev. Cell. 2007; 13:151–159. [PubMed: 17609117]

References

35. Sokol NS, et al. *Drosophila let-7* microRNA is required for remodeling of the neuromusculature during metamorphosis. Genes Dev. 2008; 22:1591–1596. [PubMed: 18559475]
36. Caldwell JC, Fineberg SK, Eberl DF. *reduced ocelli* encodes the leucine rich repeat protein *Pray For Elves* in *Drosophila melanogaster*. Fly. 2007; 1:146–152. [PubMed: 18820435]
37. Hime GR, Brill JA, Fuller MT. Assembly of ring canals in the male germ line from structural components of the contractile ring. J. Cell Sci. 1996; 109:2779–2788. [PubMed: 9013326]
38. Harrison DA, McCoon PE, Binari R, Gilman M, Perrimon N. Drosophila unpaired encodes a secreted protein that activates the JAK signaling pathway. Genes Dev. 1998; 12:3252–3263. [PubMed: 9784499]
39. Bailey TL, Elkan C. Fitting a mixture model by expectation maximization to discover motifs in biopolymers. Proc. Int. Conf. Intell. Syst. Mol. Biol. 1994; 2:28–36. [PubMed: 7584402]
40. Schmittgen TD, Livak KJ. Analyzing real-time PCR data by the comparative C_T method. Nature Protocols. 2008; 3:1101–1108. [PubMed: 18546601]
41. Min KJ, Yamamoto R, Buch S, Pankratz M, Tatar M. *Drosophila* lifespan control by dietary restriction independent of insulin-like signaling. Aging Cell. 2008; 7:199–206. [PubMed: 18221413]
42. Yuan JS, Reed A, Chen F, Stewart CN Jr. Statistical analysis of real-time PCR data. BMC Bioinformatics. 2006; 7:85. [PubMed: 16504059]
43. Brennecke J, et al. Discrete small RNA-generating loci as master regulators of transposon activity in *Drosophila*. Cell. 2007; 128:1089–1103. [PubMed: 17346786]
44. Haley B, Zamore PD. Kinetic analysis of the RNAi enzyme complex. Nature Struct. Mol. Biol. 2004; 11:599–606. [PubMed: 15170178]
45. Haley B, Foys B, Levine M. Vectors and parameters that enhance the efficacy of RNAi-mediated gene disruption in transgenic *Drosophila*. Proc. Natl Acad. Sci. USA. 2010; 107:11435–11440. [PubMed: 20534445]

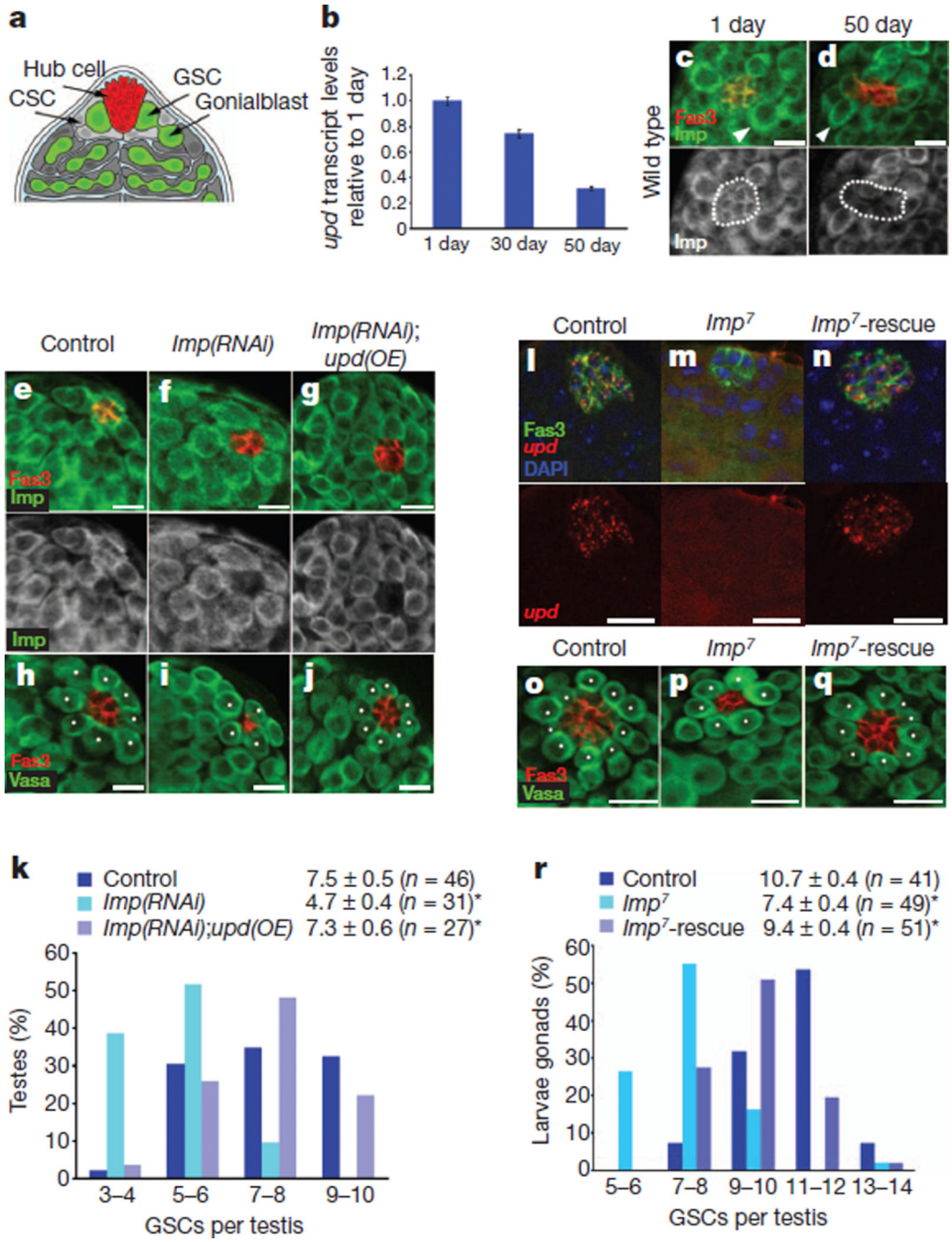

Figure 1. Imp regulates upd levels and GSC maintenance in the testis

a, The apical tip of a *Drosophila* testis. CSC, cyst stem cell. **b**, *upd* mRNA decreases with age (qRT–PCR). One representative experiment is shown ($n = 3$); error bars denote s.d. of triplicate measurements. **c**, **d**, Testes from 1-day-old (**c**) or 50-day-old (**d**) flies immunostained for Imp (green) and Fas3 (red, hub). Note reduced Imp levels in hub cells of aged males (dotted lines, bottom panels) compared with a modest reduction in GSCs (arrowheads, top panels). **e–j**, Overexpression (OE) of *upd* suppresses the loss of GSCs owing to the loss of *Imp*. Staining for Imp (green) to confirm knockdown (**e–g**) or for the

germline marker Vasa (green) (**h–j**). White dots in **h–j** denote GSCs. Genotypes: control, *w*$^{-}$*, upd-GAL4, UAS-gfp* outcrossed to *w*^{1118}*; Imp(RNAi), w*$^{-}$*, upd-GAL4, UAS-gfp; UAS-Imp(RNAi); Imp(RNAi);upd(OE), w*$^{-}$*, upd-GAL4, UAS-gfp; UAS-Imp(RNAi); UAS-upd, TM2*. **k**, GSC distribution as in **h–j**. **l–q**, L3 male gonads stained for Fas3 (green) and *upd* (red) (**l–n**) or Fas3 (red) and Vasa (green) (**o–q**). Nuclei in **l–n** were counterstained blue with 4′,6-diamidino-2-phenylindole (DAPI). White dots in **o–q** denote GSCs. Genotypes: control, EP(X)760; *Imp*^{7}*; Imp*^{7}-rescue, *Imp*^{7}/Y; *8-156-GAL4; UAS-Imp*^{T21}. **r**, GSC distribution as in **o–q**. The mean ± 95% confidence interval are shown in **k** and **r**. **P* < 0.01 compared with controls (Student's *t*-test). Scale bars, 10 μm.

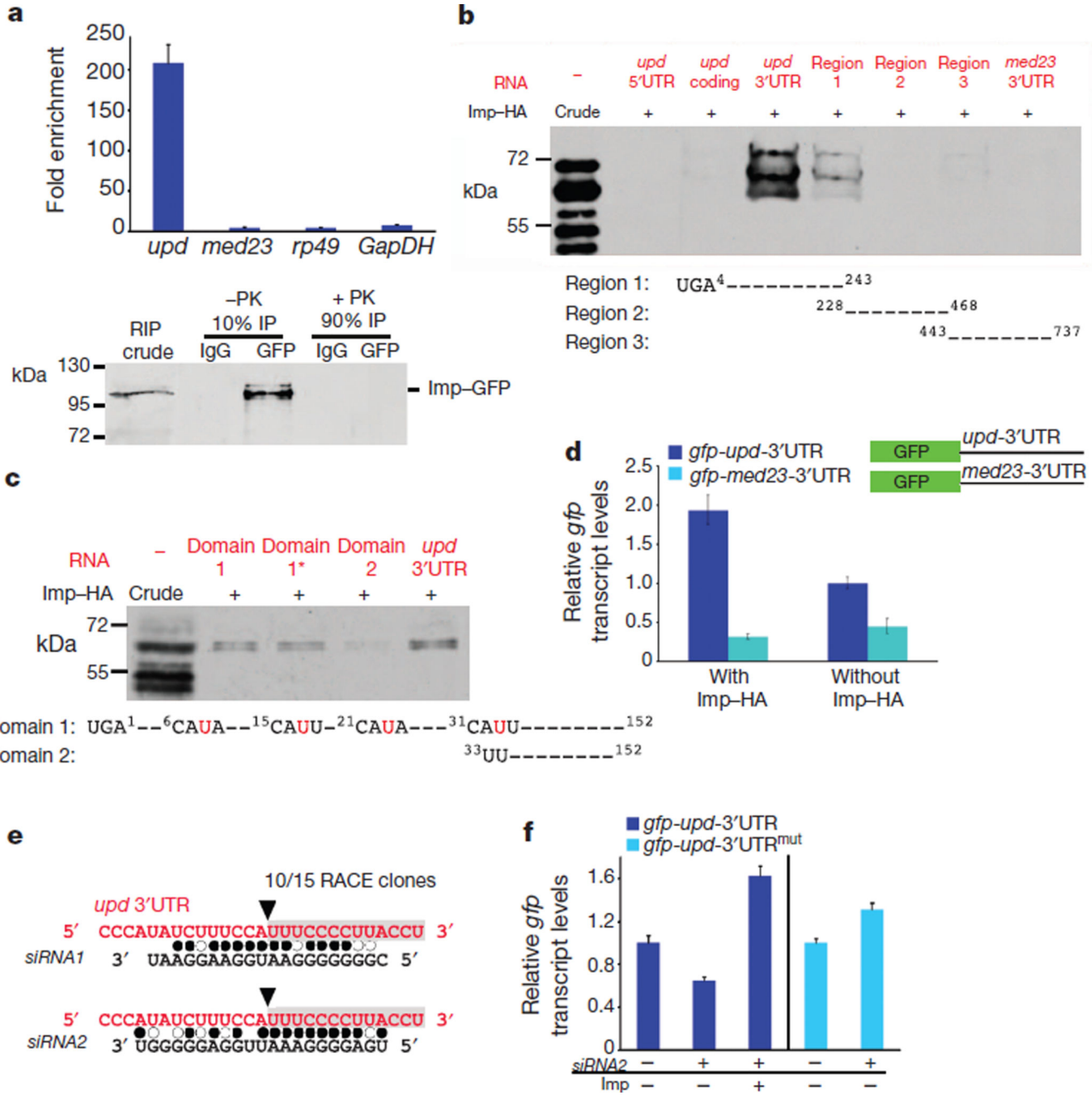

Figure 2. Imp binds to upd mRNA and counteracts siRNA-mediated degradation

a, Top, fold-enrichment of the indicated mRNAs after RNA immunoprecipitation (RIP) with anti-GFP antibodies relative to control IgG from the testes of young Imp–GFP flies. Bottom, immunoblot for Imp–GFP. Ten per cent of the immunoprecipitate was used to confirm immunoprecipitation efficiency; the remaining 90% was treated with proteinase K (PK) and used for qRT–PCR. **b**, **c**, *In vitro* protein–RNA binding assay. Top panels, immunoblots for Imp–HA binding to designated RNA fragments. Imp–HA binds to region 1 of the *upd* 3′UTR (**b**), and to domain 1 and 1* within region 1 of the *upd* 3′UTR, but not to domain 2 (**c**). Mutations in domain 1* of the *upd* 3′UTR are indicated in red (**c**). **d**, qRT–PCR showing

relative *gfp* mRNA levels in cells co-transfected with actin-*GAL4* and the indicated *gfp* reporter constructs. Expression of *gfp* is presented relative to cells without Imp–HA and is normalized to *GAL4*. Note that *gfp-upd*-3′UTR mRNA is sixfold higher than *gfp-med23*-3′UTR in cells expressing Imp–HA. **e**, Sequence of cleavage product from aged testes identified a fragment starting at nucleotide 33 within the *upd* 3′UTR (black arrowhead, grey box). Alignment of the *upd* 3′UTR with endo-siRNAs found in aged testis library. Filled circles, canonical base pairing; open circles, GU pairs. **f**, qRT–PCR showing *gfp* fromS2 cells transfected with *gfp-upd*-3′UTR or with *gfp-upd*-3′UTR^{mut} (^{32}AUU = CGG), with or without Imp and *siRNA2*. Levels normalized to *rp49* and relative to control *gfp* levels without *siRNA2*. Error bars in **a**, **d** and **f** denote s.d. of triplicate measurements.

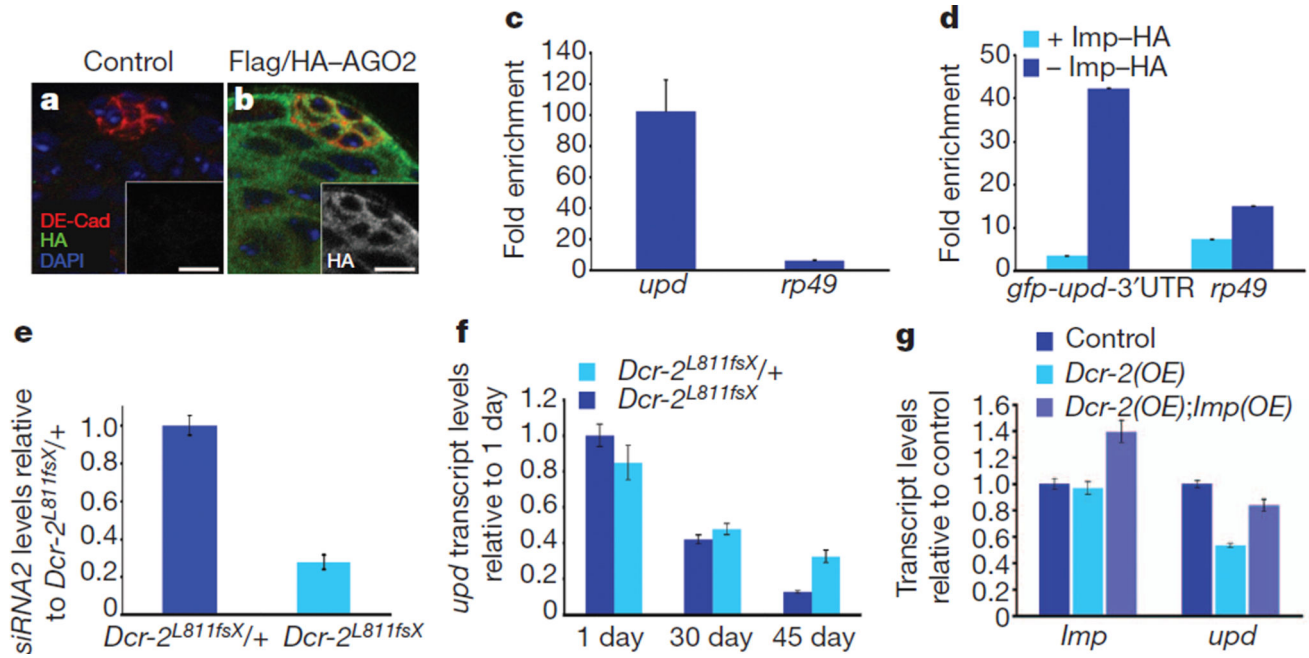

Figure 3. Imp counteracts AGO2 and Dicer-2 to regulate upd levels and stem-cell maintenance

a, **b**, Testes from control (**a**) or Flag/HA–AGO2 (**b**) males showing AGO2 expression throughout the testis tip. DE-Cad, *Drosophila* E-cadherin. Scale bars, 10 μm. **c**, Flag/HA–AGO2 RNA immunoprecipitation from the testes of 30-day-old males. The fold enrichment of *upd* or *rp49* RNA bound to mouse anti-Flag relative to control IgG is shown. **d**, qRT–PCR after Flag–AGO2 RNA immunoprecipitation from S2 cells, showing fold enrichment of *gfp-upd*-3′UTR or *rp49* RNA bound to anti-Flag antibodies relative to control IgG, in the presence (light blue) or absence (dark blue) of Imp–HA. **e**, qRT–PCR showing mature *siRNA2* levels relative to *bantam* in testes from $Dcr\text{-}2^{L811fsX}/+$ heterozygous and $Dcr\text{-}2^{L811fsX}$ homozygous flies. Expression normalized to heterozygotes. Note the 72% reduction in *siRNA2* levels in $Dcr\text{-}2^{L811fsX}$ homozygous flies. **f**, qRT–PCR of *upd* levels in testes from $Dcr\text{-}2^{L811fsX}/+$ and $Dcr\text{-}2^{L811fsX}$ flies measured in testes from 1-, 30- and 45-day-old males; shown are *upd* levels relative to levels in 1-day-old *Dcr-2* heterozygotes. **g**, qRT–PCR showing mRNA abundance for *Imp* and *upd* relative to controls. Note reduction of *upd* transcript levels in flies expressing ectopic *Dcr-2*, which is suppressed by co-expression of *Imp*. mRNA levels in **f** and **g** were normalized to *GapDH*. Error bars in **c–g** denote s.d. of triplicate measurements.

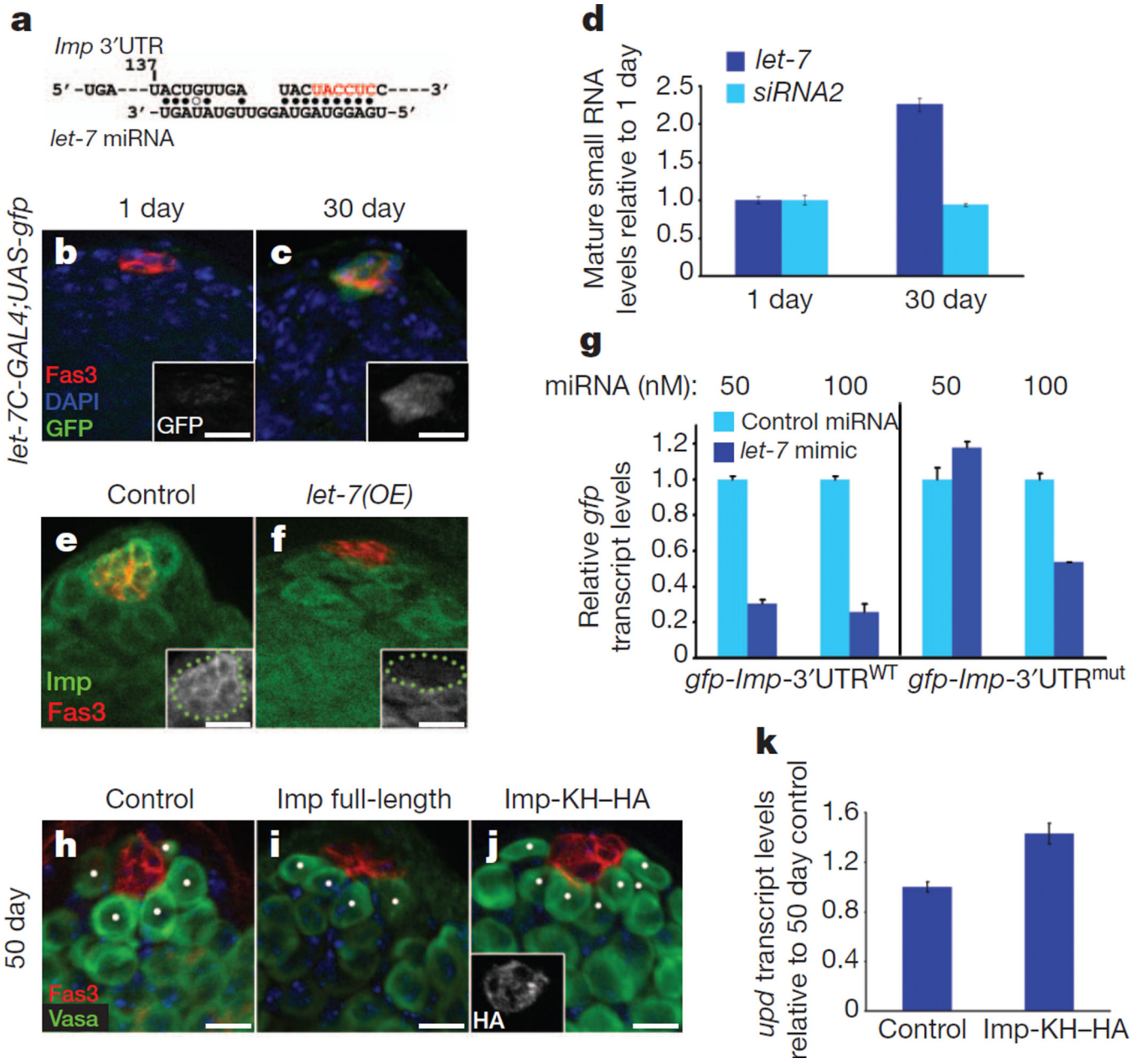

Figure 4. Imp is targeted by let-7 miRNA in the testis

a, Canonical *let-7* seed sequence within the *Imp* 3′UTR. Start site at position 137. Filled circles, canonical base pairs; open circles, GU base pairs. Note perfect seed pairing of nucleotides 2–7 with the 5′end of *let-7* (red). **b**, **c**, Testes from1-day-old (**b**) and 30-day old (**c**) males immunostained for GFP (green, insets) to follow *let-7C* expression. **d**, qRT–PCR for mature *let-7* and *siRNA2* relative to *bantam* in the testes of 1- and 30-day-old males. Levels normalized to 1-day-old adults. **e**, **f**, Overexpression of *let-7* in hub cells reduces Imp expression. Larval testes immunostained as indicated. Green dots in insets outline hub cells. Genotypes: control, *upd-GAL4*$^{-}$*;TM3, kr-GAL4, UAS-gfp* (**e**); *let-7(OE), upd-GAL4; UASlet-7*$^{701.12.9}$ (**f**). **g**, *let-7* targets a *gfp-Imp*-3′UTR reporter in S2 cells. qRT–PCR for *gfp*

transcript levels relative to control miRNA at the same concentration. Transfection of 50 nM *let-7* mimic results in a 70% reduction in the *gfp* transcript of *gfp-Imp*-3′UTR^{WT} but not of *gfp-Imp*-3′UTR^{mut} (mutated bases to disrupt *let-7* binding are coloured red in **a**). Higher concentrations of *let-7* target the *Imp* 3′UTR through additional sites. **h–j**, Immunofluorescence of testes from 50-day-old control (**h**), Imp full-length (**i**) or Imp with a truncated 3′UTR (Imp-KH–HA; **j**). Genotypes: control, *w, upd-GAL4, UAS-gfp* outcrossed to w^{1118} (**h**); Imp full-length, w^{-}*, upd-GAL4, UAS-gfp;* $UASImp^{T21}$ (**i**); Imp-KH–HA, *w, upd-GAL4;* $UAS\text{-}Imp^{HA\text{-}KH1\text{-}3\text{-}3}$ (**j**). Scale bars, 10 μm. **k**, qRT–PCR showing relative *upd* levels in testes from 50-day-old males. Control and Imp-KH–HA genotypes are as in **h** and **j**, respectively. Note the 1.5-fold increase in *upd* levels in aged flies overexpressing the Imp-KH–HA transgene. *gfp* and *upd* mRNA expression in **g** and **k** are shown relative to controls and normalized to *GapDH*.